

# NJC

Accepted Manuscript



This is an *Accepted Manuscript*, which has been through the Royal Society of Chemistry peer review process and has been accepted for publication.

*Accepted Manuscripts* are published online shortly after acceptance, before technical editing, formatting and proof reading. Using this free service, authors can make their results available to the community, in citable form, before we publish the edited article. We will replace this *Accepted Manuscript* with the edited and formatted *Advance Article* as soon as it is available.

You can find more information about *Accepted Manuscripts* in the [Information for Authors](#).

Please note that technical editing may introduce minor changes to the text and/or graphics, which may alter content. The journal's standard [Terms & Conditions](#) and the [Ethical guidelines](#) still apply. In no event shall the Royal Society of Chemistry be held responsible for any errors or omissions in this *Accepted Manuscript* or any consequences arising from the use of any information it contains.

# Synthesis and Conformational Studies of a Stable Peptidomimetic $\beta$ -Hairpin Based on a Bifunctional Diketopiperazine Turn Inducer.

Cite this: DOI: 10.1039/x0xx00000x

Received 00th January 2012,  
Accepted 00th January 2012

DOI: 10.1039/x0xx00000x

www.rsc.org/

Leila Vahdati,<sup>a,b</sup> Roberto Fanelli,<sup>a</sup> Guillaume Bernadat,<sup>b</sup> Isabel Correia,<sup>c</sup> Olivier Lequin,<sup>c</sup> Sandrine Onger, <sup>\*b</sup> and Umberto Piarulli <sup>\*a</sup>

The design, synthesis and conformational studies of a new  $\beta$ -hairpin mimic, **2**, are described in this paper. The design towards hairpin **2** is based on the assembly of the bifunctional DKP-**1** as a  $\beta$ -turn inducer, a peptidomimetic strand, namely 5-amino-2-methoxybenzhydrazide, to stabilize the formation of  $\beta$ -sheets, and finally a tetrapeptide sequence, GVVV, containing the hydrophobic residues Val, Ile and Gly. The synthesis of hairpin **2** was performed in solution while the formation of the  $\beta$ -hairpin in protic solvents was proven by NMR investigations (<sup>1</sup>H and <sup>13</sup>C chemical shifts, vicinal coupling constants and ROEs) and corroborated by computational studies (Monte-Carlo conformational search, molecular dynamics and DFT calculations).

## Introduction

In the field of peptidomimetic foldamers, much effort has been focused on the design and synthesis of conformationally constrained compounds that mimic or induce specific secondary structural features of peptides and proteins.<sup>1</sup> In fact, short linear peptides are inherently flexible molecules, especially in aqueous solution, and as such are often poor mimics of the secondary structures (turns,  $\alpha$ -helices,  $\beta$ -sheets) found on the surfaces of folded proteins. In particular,  $\beta$ -sheets are ubiquitous in protein tertiary and quaternary structure, and are involved in protein dimerization and oligomerization, protein-protein interaction, and peptide and protein aggregation.<sup>2</sup> The formation of peptide and protein aggregates through the interaction of  $\beta$ -sheets has increasingly drawn attention since it occurs in many widespread human diseases, such as AIDS, cancer, Alzheimer's disease, prion diseases, and other amyloid-related diseases. In the case of amyloid-related diseases, the protein aggregation process involves a secondary structure transition from unordered/ $\alpha$ -helix to  $\beta$ -sheet conformation, leading to cross  $\beta$ -sheet structure formation with  $\beta$ -strands perpendicular to the long fibril axis.<sup>3</sup>  $\beta$ -Strands interact through edge-to-edge hydrogen bonding to form extended layers and through face-to-face hydrophobic or van der Waals interactions to form layered sandwich-like structures.<sup>4</sup> Besides backbone hydrogen bonding, side chains from adjacent layers can form hydrophobic contacts or knob-hole interactions.

Several approaches have been used to inhibit the aggregation of proteins, either by stabilizing native conformations or by

preventing  $\beta$ -strand intermolecular interactions using  $\beta$ -sheet binders.<sup>5</sup> Natural and synthetic  $\beta$ -hairpins,<sup>6</sup> and more recently macrocyclic  $\beta$ -sheet mimic structures,<sup>7</sup> have been designed and used as  $\beta$ -sheet binders and inhibitors of aggregation. In these structures, two peptide sequences or one peptide and one peptidomimetic are held together in a suitable position to form two interacting  $\beta$ -strands by the use of a reverse-turn mimic where the peptide chain folds back upon itself, or forcing them into cyclic derivatives. One of the two strands is normally composed of amino acid residues important for stabilizing intra- and intermolecular interactions involved in aggregation and amyloid formation.

Recently, some of us reported a bifunctional diketopiperazine (DKP) scaffold **1** (Figure 1) derived from L-aspartic acid and (S)-2,3-diaminopropionic acid, bearing the amino and carboxylic acid functionalities in a *cis* relationship.<sup>8</sup> As such, this derivative can be seen as  $\beta$ -turn mimic and promoter of antiparallel  $\beta$ -sheets.

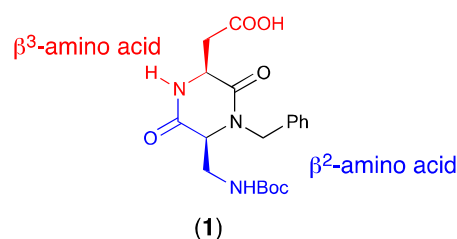


Figure 1 Structure of the bifunctional diketopiperazine scaffold **1** (DKP-**1**) highlighting the conformationally constrained  $\beta^2$ - $\beta^3$  dipeptide sequence

DKP-1 was introduced into peptidic sequences and their conformation investigated by NMR and computational studies revealing the formation of  $\beta$ -hairpin mimics involving 10-membered H-bonded rings and a reverse turn of the growing peptide chain.<sup>8a</sup> The same conformation was observed in oligomers of DKP-1, mimicking  $\beta$ -bend-ribbon structures.<sup>9</sup>

In this paper we report the synthesis and the conformational studies of the acyclic  $\beta$ -hairpin mimic **2**, where DKP-1 is linked to a peptidomimetic and a tetrapeptidic arm.

## Results and Discussion

Our design towards a stable hairpin **2** (Figure 2), which could interact and eventually act as a  $\beta$ -sheet binder and aggregation inhibitor, involved assembling the bifunctional DKP-1 mentioned above, a peptidomimetic strand to stabilize the formation of  $\beta$ -sheets and finally a suitable peptide sequence for binding to the aggregating protein. Although DKP-1 is able to stabilize hairpin structures when introduced between two peptide sequences,<sup>8a</sup> the choice to substitute one of the peptide sequences by a peptidomimetic strand was aimed at increasing the resistance to proteolysis of the molecule *vis a vis* of its potential use in biological assays as proyein aggregation inhibitor. As peptidomimetic strand, we decided to incorporate into our sequence 5-amino-2-methoxybenzhydrazide, which is a part of the  $\beta$ -strand mimic ("Hao" unit) reported by Nowick and co-workers.<sup>10</sup> The introduction of 5-amino-2-methoxybenzhydrazide into  $\beta$ -strand mimics was shown, by some of us, to be extremely effective in the formation of intermolecular  $\beta$ -sheets with the terminal parts of HIV-1 proteases and in the inhibition of their dimerization, as well as

to increase the proteolytic stability with respect to proteases.<sup>11</sup> Finally, as for the peptide sequence, four residues were introduced, chosen from the classical hydrophobic residues (Val, Ile, Gly) encountered in natural  $\beta$ -sheet structures, and in particular in the hydrophobic sequences playing a crucial role in promoting and stabilizing the protein aggregation.<sup>12</sup>

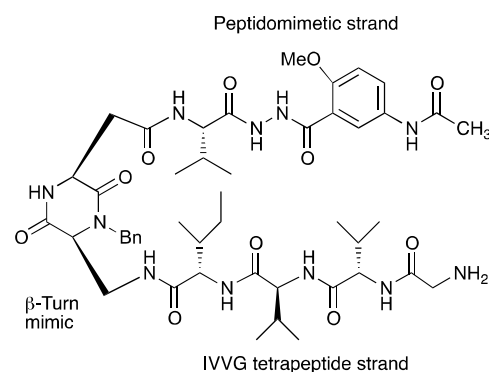
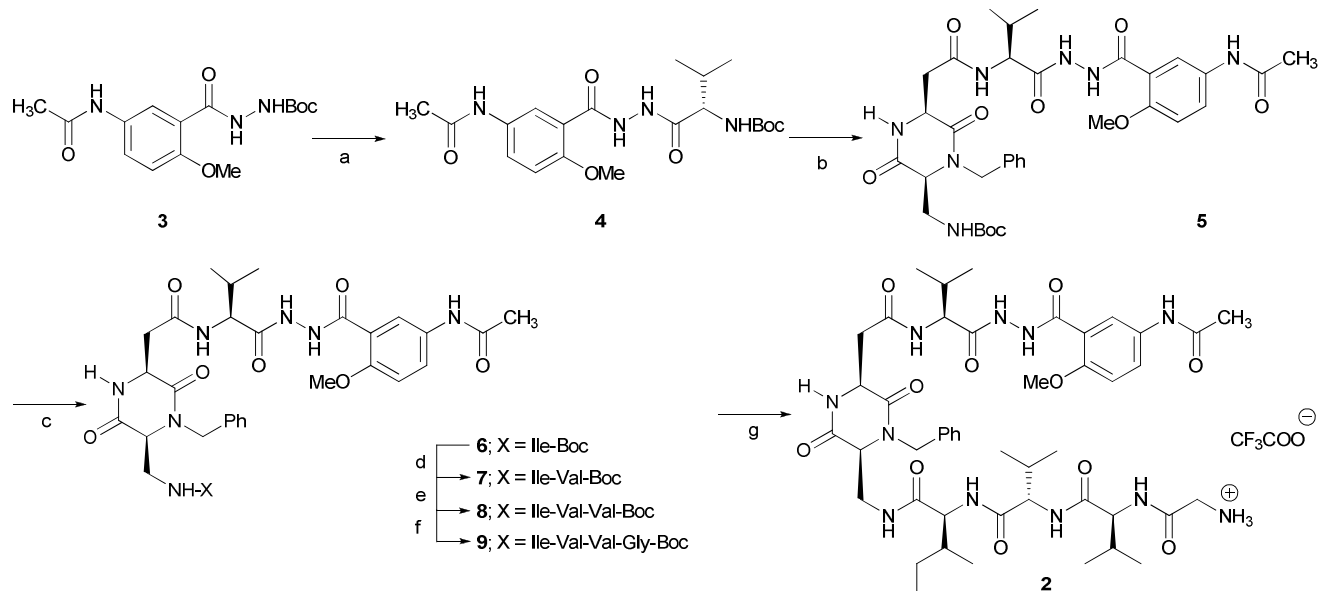


Figure 2. Structure of  $\beta$ -hairpin mimic **2**, highlighting the peptidic, peptidomimetic and  $\beta$ -turn mimic components.

## Synthesis

The synthesis of hairpin **2** was conveniently realized according to Scheme 1. Boc-5-amino-2-methoxy benzhydrazide **3** was prepared according to a published procedure. **Error. II segnalibro non è definito.** Treatment of **3** with TFA and coupling to Boc-Val-OH afforded the peptidomimetic strand **4** in good yield.



Scheme 1. Synthesis of hairpin **2**. (a) TFA,  $\text{CH}_2\text{Cl}_2$ , 0 °C, 2h; Boc-Val-OH, HBTU, HOBT, DIPEA, DMF, room temperature, 24h; (b) TFA,  $\text{CH}_2\text{Cl}_2$ , 0 °C, 2h; **1**, DMTMM( $\text{BF}_4$ ), NMM, DMF, 0 °C to room temperature, overnight; (c) TFA,  $\text{CH}_2\text{Cl}_2$ , 0 °C, 1h; HATU, HOAt, DIPEA, Boc-Ile-OH, DMF, 0 °C to room temperature, overnight; (d) TFA,  $\text{CH}_2\text{Cl}_2$ , 0 °C, 1h; HATU, HOAt, DIPEA, Boc-Val-OH, DMF, 0 °C to room temperature, overnight; (e) TFA,  $\text{CH}_2\text{Cl}_2$ , 0 °C, 1h; HATU, HOAt, DIPEA, Boc-Val-OH, DMF, 0 °C to room temperature, overnight; (f) TFA,  $\text{CH}_2\text{Cl}_2$ , 0 °C, 1h; HATU, HOAt, DIPEA, Boc-Gly-OH, DMF, 0 °C to room temperature, overnight; (g) TFA,  $\text{CH}_2\text{Cl}_2$ , 0 °C, overnight.

## PAPER (or FOCUS or PERSPECTIVE)

After Boc deprotection, the peptidomimetic strand was ready for chain elongation with the *cis*-DKP-1 hairpin mimic, prepared according to a procedure developed in our laboratories.<sup>8c</sup> Unfortunately the coupling reaction between the scaffold DKP-1 and the peptidomimetic strand provided compounds **5** in a poor yield (< 20%) using the common coupling reagents for sterically hindered systems, such as HATU and HOAt. An investigation of alternative coupling agents was then undertaken: HOBt/EDC.HCl or 4-(4,6-dimethoxy-1,3,5-triazin-2-yl)-4-methylmorpholinium chloride [DMTMM(Cl)] both in DMF and DCM afforded the desired compound in a somewhat erratic way, and in low yield (34 and 25%, respectively). On the other hand, cyanuric chloride with N-methylmorpholine or DIPEA<sup>13</sup> as a base did not lead to the formation of the compound.<sup>14</sup> Satisfactory results were obtained with the triazine-based reagent DMTMM(BF<sub>4</sub>) in the presence of N-methylmorpholine in DMF,<sup>15</sup> which was successfully used for the coupling of natural and unnatural sterically hindered amino acids and for fragment condensation. In this way, the coupling product **5** was obtained in a 45% yield.

The construction of the lower peptidic arm was then performed via solution peptide synthesis using Boc protected amino acids. In each coupling step, the Boc protected amino acid was introduced using HATU and HOAt in DMF, leading to the formation of the expected compound in high yields.

### NMR Conformational analysis

As we anticipated in the introduction, diketopiperazine scaffold **1** can be seen as a conformationally constrained dipeptide formed by a  $\beta^2$  and a  $\beta^3$ -amino acid (see Figure 1). Extensive investigation on  $\beta$ -peptides indicated that these are able to adopt stable secondary structures such as helices and sheets.<sup>16</sup> In particular, the stabilization of  $\beta$ -peptide-hairpins sequences was shown to occur in oligo- $\beta$ -peptides containing the dipeptide sequence formed by a  $\beta^2$ -amino acid (C2-substituted) followed by a  $\beta^3$ -amino acid (C3-substituted).<sup>17</sup> The intramolecular hydrogen bonding pattern involves the formation of a 10-membered H-bonded ring between the C=O of the  $\beta^3$ -amino acid and the NH of the  $\beta^2$ -amino acid. The same structural feature was observed when DKP-1 was introduced in short peptide sequences (e.g. Val-Ala-DKP-1-Val-Ala)<sup>8</sup> or in foldamers composed of repeating units of DKP-1.<sup>9</sup> In the case of compound **2**, the use of a longer peptide sequence on one arm and of a  $\beta$ -strand peptidomimetic, which was reported to act mainly in constrained cyclic structure, did not grant the formation of a stable hairpin.

The conformation of **2** was analysed in a protic solvent, which is more challenging for intramolecular hydrogen bond formation in comparison with aprotic organic solvents such as

chloroform. Unfortunately, **2** turned out to be poorly soluble in aqueous solution but could be solubilised in methanol at millimolar concentrations.

Complete <sup>1</sup>H and <sup>13</sup>C resonance assignments were obtained from the analysis of 2D <sup>1</sup>H-<sup>1</sup>H TOCSY and ROESY, and 2D <sup>1</sup>H-<sup>13</sup>C HSQC and HMBC experiments (Table 1). Most experiments were recorded at 298 K as the <sup>1</sup>H spectra exhibited good chemical shift dispersion at this temperature. However the hydrazide proton NH<sub>b</sub> showed a broad signal and NH<sub>c</sub> was broadened beyond detection. Cooling the sample down to 270 K gave rise to peak sharpening of hydrazide protons and in particular the NH<sub>c</sub> proton could be observed. Notably, weak additional resonances could be detected on the spectra, corresponding to a second set of chemical shifts. This minor species, representing less than 5%, turns out to be in equilibrium with the major form, as exchange peaks were observed on 2D ROESY spectra between the NH protons of two forms. The origin of this exchange phenomenon was not characterized but could be due to a rotation of 180° about the Ar-NH or Ar-CO bonds, occurring in slow exchange on the <sup>1</sup>H NMR time scale.

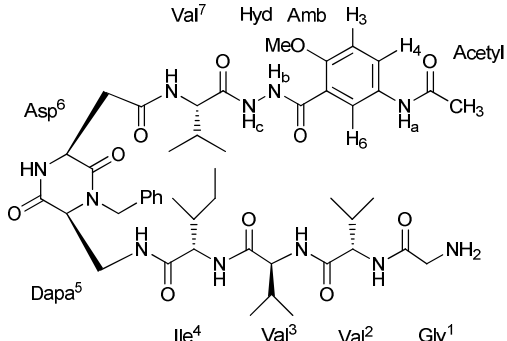
The conformational analysis of **2** was based on <sup>1</sup>H and <sup>13</sup>C chemical shifts, vicinal coupling constants and ROEs. The <sup>1</sup>H $\alpha$  and <sup>13</sup>C $\alpha$  chemical shift deviations (CSD), defined as the differences between experimental chemical shifts and corresponding random coil values, are good descriptors of backbone conformational space for each residue.<sup>18</sup> All Val and Ile residues are characterized by downfield shifted H $\alpha$  protons (positive CSD values between +0.21 and +0.78 ppm) and upfield shifted C $\alpha$  carbons (negative CSD values between -4.4 and -2.5 ppm), indicating that extended conformations predominate (Table 2).

**Table 2.** Chemical shift deviations (CSD) of aliphatic residues of **2** in methanol

Residue	NH (ppm)	H $\alpha$ (ppm)	C $\alpha$ (ppm)
Val <sup>2</sup>	0.41	0.43	-2.5
Val <sup>3</sup>	0.66	0.21	-2.5
Ile <sup>4</sup>	0.55	0.49	-2.6
Val <sup>7</sup>	0.55	0.78	-4.4

The vicinal <sup>3</sup>J<sub>HN-H $\alpha$</sub>  coupling constant also yields direct information on the main chain  $\phi$  dihedral angle, through the Karplus relationship. The coupling constants of the four aliphatic residues (Table 3) exhibit large values (8.8–9.4 Hz range), reflecting  $\phi$  angle values around -120°, as expected for  $\beta$ -strand conformations.

## PAPER (or FOCUS or PERSPECTIVE)

**Table 1.**  $^1\text{H}$  NMR and  $^{13}\text{C}$ -NMR chemical shifts of **2** (1.4 mM) in  $\text{CD}_3\text{OH}$  at 298 K


Residue	$\delta$ NH (ppm)	$\delta$ H $^{\alpha}$ (ppm)	$\delta$ H $^{\beta}$ (ppm)	$\delta$ Other protons (ppm)	$\delta$ CO (ppm)	$\delta$ C $^{\alpha}$ (ppm)	$\delta$ C $^{\beta}$ (ppm)	$\delta$ Other carbons (ppm)
Gly <sup>1</sup>		3.78		-	167.6	42.1	-	-
Val <sup>2</sup>	8.36	4.59	2.13	$\gamma$ CH <sub>3</sub> 0.87, 0.89	173.1	59.7	32.5	$\gamma$ CH <sub>3</sub> 19.7, 18.0
Val <sup>3</sup>	8.60	4.37	1.91	$\gamma$ CH <sub>3</sub> 0.85, 0.84	173.4	59.7	32.9	$\gamma$ CH <sub>3</sub> 19.0, 19.5
Ile <sup>4</sup>	8.52	4.72	1.78	$\gamma$ CH <sub>2</sub> 1.55, 1.11; $\gamma$ CH <sub>3</sub> 0.89; $\delta$ CH <sub>3</sub> 0.86	174.0	58.5	38.3	$\gamma$ CH <sub>2</sub> 26.0; $\gamma$ CH <sub>3</sub> 16.2; $\delta$ CH <sub>3</sub> 11.6
Dapa <sup>5</sup>	8.67	4.09	3.85, 3.76	CH <sub>2</sub> 5.39, 3.98; Bn ~ (7.34, 7.33, 7.31)	166.9	57.6	40.1	CH <sub>2</sub> 47.6; Bn 129.8, 129.1, 129.0, 136.5
Asp <sup>6</sup>	8.44	4.40	3.30, 2.86	-	168.3	52.8	37.8	$\gamma$ CO 171.1
Val <sup>7</sup>	8.51	4.94	2.05	$\gamma$ CH <sub>3</sub> 1.01, 1.00	169.3	57.8	32.9	$\gamma$ CH <sub>3</sub> 19.4, 19.4
NH <sub>c</sub> -NH <sub>b</sub>	11.59*, 10.83			-				
Amb	9.82 (Ha)			H <sub>3</sub> 7.18; H <sub>4</sub> 7.88; H <sub>6</sub> 8.22; OCH <sub>3</sub> 4.03	162.8			C <sub>1</sub> 120.2; C <sub>2</sub> 155.2; C <sub>3</sub> 113.5; C <sub>4</sub> 127.0; C <sub>5</sub> 133.9; C <sub>6</sub> 124.2; OCH <sub>3</sub> 57.1
Acetyl				CH <sub>3</sub> 2.13	171.5			CH <sub>3</sub> 23.9

\* Observed at 270.4 K only

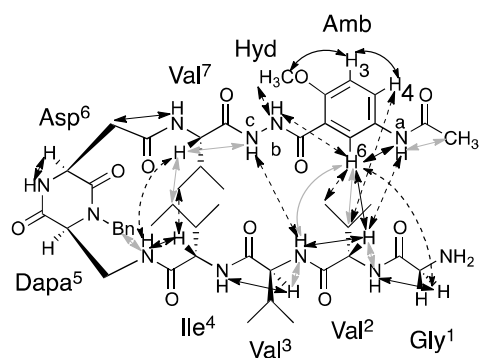


Figure 3. Chemical structure of **2** showing the assigned ROEs. ROE cross-peaks were integrated to extract interproton distances and were grouped into three classes: black plain arrows, distances below 2.8 Å; grey plain arrows, distances between 2.8 and 3.8 Å; dashed arrows, distances above 3.8 Å. Residue abbreviations: Amb, 5-amino-2-methoxybenzoyl; Dapa = 2,3-diaminopropionic acid; Hyd, hydrazide.

Finally, the analysis of H $\alpha$ -HN ROE correlations (Fig. 3) reveals strong sequential and medium intraresidual H $\alpha$ -HN ROEs, which is characteristic of extended backbone conformations. Evidence for the formation of a  $\beta$ -hairpin came from the observation of numerous long-range ROEs between the two  $\beta$ -strands. Indeed, 11 interstrand ROEs could be detected, involving both backbone and sidechain protons (Fig. 3). The set of ROEs indicates that Ile<sup>4</sup> and Val<sup>7</sup> residues face together and that Val<sup>2</sup> makes contacts with the aromatic ring.

A weak ROE observed between the hydrazide proton NH<sub>c</sub> and Val<sup>3</sup> amide proton further supports the formation of an antiparallel  $\beta$ -sheet, the anomalously low intensity being due to the short transverse relaxation time of NH<sub>c</sub> proton.

A close inspection of ROE-derived distances revealed the existence of preferred conformers of hydrazide/amide bonds on either side of the aromatic unit. The distances between NH<sub>a</sub> and H<sub>4</sub>, H<sub>6</sub> protons are consistent with the preferred orientation of the acetamido group depicted in Fig. 3. Furthermore, the ROE between hydrazide NH<sub>b</sub> proton and methoxy protons supports

the formation of a hydrogen bond between the two groups (Fig. 3). Finally, the long-range ROE between the aromatic H<sub>6</sub> proton and the Gly<sup>1</sup> H $\alpha$  protons is not expected in a regular  $\beta$ -sheet and can be ascribed to fraying at the N-terminus of the  $\beta$ -strand.

We next examined the temperature dependence of amide proton chemical shifts as it can provide information on the network of hydrogen bonds and their relative stabilities (Table 3).

**Table 3.** Temperature coefficients and coupling constants for NH protons of **2** in methanol

Residue	$\Delta\delta/\Delta T$ (ppb/K)	J ( $\pm 0.3$ Hz)
Val <sup>2</sup>	-6.5	8.8
Val <sup>3</sup>	-6.0	9.2
Ile <sup>4</sup>	-9.4	9.4
Dapa <sup>5</sup>	-4.2	3.8
Asp <sup>6</sup>	-8.2	<2
Val <sup>7</sup>	-8.2	9.4
NH <sub>a</sub>	n.d.	bs*
NH <sub>b</sub>	-4.5	bs*
NH <sub>c</sub>	-5.4	bs*

\* bs (broad signal)

Amide protons that are engaged in intramolecular hydrogen bonds typically exhibit small temperature dependence ( $\Delta\delta_{\text{HN}}/\Delta T > -4.5$  ppb/K) in aqueous<sup>19</sup> and alcoholic solvents<sup>20</sup> while those that are not intramolecularly hydrogen-bonded usually exhibit largely negative values of their temperature coefficients. The amide protons of Ile<sup>4</sup>, Asp<sup>6</sup> and Val<sup>7</sup> exhibit the strongest variations, as expected for solvent-exposed groups. In contrast, the NH<sub>b</sub> and NH<sub>c</sub> protons near the aromatic unit, together with the amide proton of Dapa<sup>5</sup>, have the smallest variations. However these temperature coefficients tend to be slightly higher than expected and that of Val<sup>3</sup> amide proton falls within intermediate values. Altogether this analysis suggests a partial engagement in intramolecular hydrogen bonds and is indicative of an equilibrium between the major  $\beta$ -hairpin conformation and minor open conformations.

Finally, we investigated whether the stabilization of the  $\beta$ -sheet conformation could result from intermolecular association at high concentration. The comparison of 1D <sup>1</sup>H spectra recorded at 1.4 mM and 80  $\mu$ M concentrations does not show significant changes in chemical shifts and linewidths, ruling out the possibility of aggregation in the mM range.

### Computational studies

Molecular modelling was employed in order to evaluate the propensity of compound **2** to adopt a hairpin structure in water. A Monte-Carlo conformational search using OPLS\_2005 molecular mechanics force field with an implicit GBSA solvation model<sup>21</sup> yielded an initial hairpin-like geometry of this molecule. Stability of this structure was further studied by molecular dynamics and DFT calculations.

Although the open end of the molecule seemed to fluctuate (in agreement with the conclusions from the NMR studies), the overall hairpin structure of the compound (evaluated by the

lifetime of key hydrogen bonds, see Figure 4) exhibited rather good stability.

Delightfully, completely extended conformations were observed several times over the course of the dynamics, with coexistence of the 4 key hydrogen bonds and formation of the expected 10, 14, 10 and 14-membered pseudoring (Figure 5). The hydrogen bond network and the dihedral angles for the  $\beta^2$  and  $\beta^3$ -aminoacids ( $\theta = -62$  and  $61^\circ$  respectively), indicate that the hairpin geometry observed in **2** is in agreement with previous examples of hairpins<sup>8</sup> and foldamers<sup>9</sup> of DKP-1.

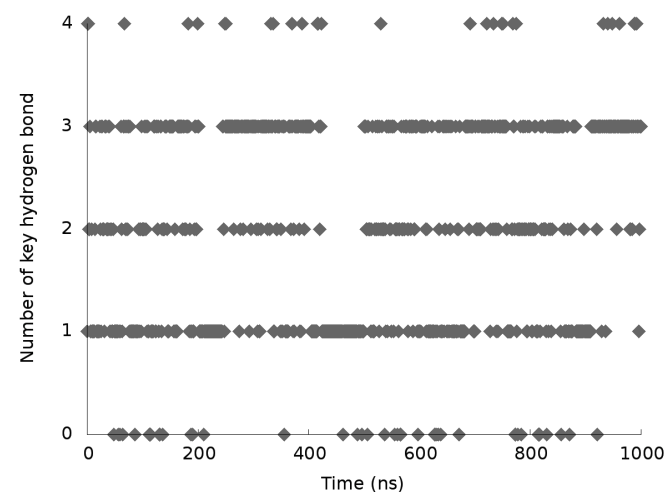


Figure 4. Evolution of the number of key hydrogen bonds for the hairpin structure over the molecular dynamics trajectory (1  $\mu$ s)

Average angle and distance values over the molecular dynamics trajectory were found in good agreement with coupling constants and ROE intensities measured (see supporting information).

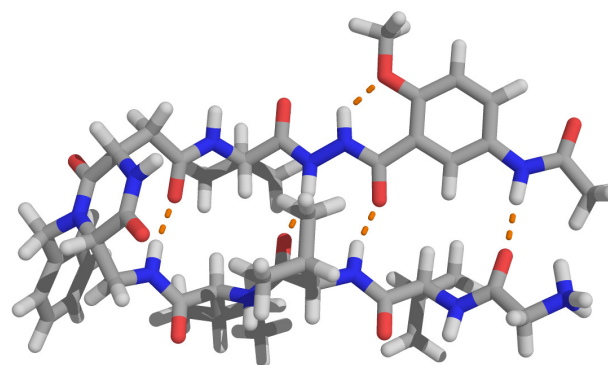


Figure 5. Hairpin structure of **2** observed during OPLS\_2005/GBSA molecular dynamics in water and refined at the B3LYP/6-31G\* level.

A discrepancy existed between the average distance from H<sup>6</sup> proton belonging to the 5-acetamido-2-methoxy benzohydrazide moiety to H<sup>a</sup> in Val<sup>2</sup> residue and the strength of the corresponding signal on the ROESY spectrum. However, this result can be accounted for by the locally dynamic character of the molecule, since 10% of the time, this distance

actually drops below 2.8 Å. This study indicated that extrapolation of major structural characteristics found by NMR in methanol to aqueous conditions was a reasonably safe assumption.

## Conclusions

In summary, in this paper, the synthesis of a  $\beta$ -hairpin mimic, based on the bifunctional diketopiperazine scaffold DKP-1 as an efficient  $\beta$ -turn inducer, a peptidomimetic arm and a tetrapeptide arm was described. The formation of a stable  $\beta$ -hairpin in protic solvents was proven by NMR investigations and corroborated by computational studies. This work provides a proof that DKP-1 is able to stabilize  $\beta$ -hairpins conformations in acyclic structures notwithstanding the elongation of the arms linked to the scaffold and the replacement of a peptidic arm by a peptidomimetic arm. Pharmacomodulations of the peptidic sequence and the peptidomimetic arm can be now envisaged in order to design suitable  $\beta$ -hairpin mimics as inhibitors of specific protein-protein interactions involving  $\beta$ -sheet structures such as those encountered in protein aggregation.

## Experimental Section

### Materials and methods.

All manipulations requiring anhydrous conditions were carried out in flame-dried glassware, with magnetic stirring and under a nitrogen atmosphere. All commercially available reagents were used as received. Anhydrous solvents were purchased from commercial sources and withdrawn from the container by syringe, under a slight positive pressure of nitrogen. Reactions were monitored by analytical thin layer chromatography using 0.25 mm pre-coated silica gel glass plates (DURASIL-25 UV254) and compounds visualized using UV fluorescence, aqueous potassium permanganate or ninhydrin. Flash column chromatography was performed according to the method of Still and co-workers using Chromagel 60 ACC (40-63  $\mu$ m) silica gel. Melting points were obtained in an open capillary apparatus and are uncorrected. Proton NMR spectra were recorded on a spectrometer operating at 300 MHz or at 400.16 MHz. Proton chemical shifts are reported in ppm ( $\delta$ ) with the solvent reference relative to tetramethylsilane (TMS) employed as the internal standard. The following abbreviations are used to describe spin multiplicity: s = singlet, d = doublet, t = triplet, q = quartet, m = multiplet, br = broad signal, dd = doublet of doublet. Carbon NMR spectra were recorded on a spectrometer operating at 75 MHz or at 100.63 MHz, with complete proton decoupling. Carbon chemical shifts are reported in ppm ( $\delta$ ) relative to TMS with the respective solvent resonance as the internal standard. Infrared spectra were recorded on a standard FT-IR and peaks are reported in  $\text{cm}^{-1}$ . Elemental analyses were performed using a Perkin Elmer 2400 Series II CHNS/O Analyzer. High resolution mass spectra (HRMS) were performed on a hybrid quadrupole time of flight mass spectrometer equipped with an ESI ion source.

### Syntheses.

#### General procedure A for deprotection reactions:

To a solution of the N-Boc-protected amino acid or peptide in  $\text{CH}_2\text{Cl}_2$  (0.13 M) was added a half volume of TFA and the reaction was stirred at r.t. for 1-3 h. The solvent was evaporated, toluene (2 $\times$ ) was added followed by evaporation, and then ether was added and evaporated to afford the corresponding TFA salt.

#### General procedure B for coupling reactions:

The N-protected amino or peptide acid (3 equiv) was dissolved in DMF (0.1 M) under a nitrogen atmosphere and the solution was cooled in an ice bath. HOAt (3 equiv), HATU (3 equiv) and DIPEA (5 equiv) were then added. The solution was stirred at 0  $^\circ\text{C}$  for 1 h and then the solution of the TFA salt in DMF was added. The reaction was stirred at 0  $^\circ\text{C}$  for 30 minutes to 1 h and at r.t. overnight. Volatiles were removed under reduced pressure and the residue was diluted with EtOAc, washed with 1M  $\text{KHSO}_4$  (2 $\times$ ) or citric acid (10% solution), aqueous  $\text{NaHCO}_3$  (2 $\times$ ) and brine (1 $\times$ ), dried over  $\text{Na}_2\text{SO}_4$ , and the solvent was evaporated under reduced pressure to afford the crude product.

#### General procedure C for coupling reactions:

DMTMM ( $\text{BF}_4$ ) (1equiv) and NMM (3 equiv) were added to a solution of the N-protected amino acid in DMF (0.1 M), under a nitrogen atmosphere and at 0  $^\circ\text{C}$ . After 30 min, a solution of the TFA salt of the peptide in DMF was added and the reaction mixture was stirred at 0  $^\circ\text{C}$  for 1 h and at r.t. overnight. Volatiles were removed under reduced pressure and the residue was diluted with EtOAc and consecutively washed with 1 M  $\text{KHSO}_4$  (2 $\times$ ) or citric acid (10% solution), aqueous  $\text{NaHCO}_3$  (2 $\times$ ) and brine (1 $\times$ ), dried over  $\text{Na}_2\text{SO}_4$  and the solvent evaporated under reduced pressure to afford the crude product.

#### Compound 4:

Compound 3 (500 mg, 1.54 mmol) was deprotected according to general procedure A. The corresponding trifluoroacetate salt and Boc-Val (369.3 mg, 1.7 mmol, 1.1 equiv) were dissolved in DMF (15 mL). DIPEA (3.4 mL, 19.25 mmol, 12.5 equiv), HBTU (645 mg, 1.7 mmol, 1.1 equiv) and HOBt (229.7 mg, 1.7 mmol, 1.1 equiv) were successively added to the reaction flask. The reaction mixture was stirred under argon at room temperature for 24 h. Volatiles were then removed under reduced pressure and the residue was dissolved in EtOAc (200 mL), and washed with 10 % aqueous citric acid (50 mL), and  $\text{K}_2\text{CO}_3$  (50 mL, 10% w/w). The organic phase was dried over  $\text{Na}_2\text{SO}_4$ , filtered and concentrated under reduced pressure. The crude product was purified by flash chromatography on silica gel (EtOAc/cyclohexane 80:20). Product 4 was obtained as a white solid (453 mg, 69 %). Mp: 136-140  $^\circ\text{C}$ ;  $^1\text{H}$  NMR (400 MHz,  $\text{CDCl}_3$ )  $\delta$  12.15 (d, 1H, J=7.0 Hz), 11.42 (d, 1H, J=7.0 Hz), 8.82 (s, 1H), 8.47 (d, 1H, J=7.0 Hz), 8.11 (s, 1H), 7.02 (d, 1H, J=7.0 Hz), 5.60 (d, 1H, J=8.7 Hz), 4.79 (m, 1H), 4.08 (s,

3H), 2.19 (s, 3H), 2.02 (m, 1H), 1.48 (s, 9H), 0.88 (m, 6H);  $^{13}\text{C}$  NMR (100 MHz,  $\text{CDCl}_3$ )  $\delta$  169.0, 165.8, 158.2, 156.0, 153.6, 133.2, 125.9, 122.8, 117.8, 112.0, 79.6, 57.1, 56.6, 33.4, 28.5, 24.7, 17.9; IR  $\nu_{\text{max}}$ : 3314, 2969, 1712, 1658, 1492, 1245, 1168; MS (ESI Positive)  $m/z$  445  $[\text{M}+23]^+$ .

#### Compound 5.

Compound 4 (0.056 mmol, 1.1 equiv) was deprotected according to general procedure A. The TFA salt was then coupled to DKP-1 20 mg, 0.051 mmol, 1 equiv according to general procedure C, affording 5 (16 mg, 45%) as a white solid after purification by flash chromatography ( $\text{CH}_2\text{Cl}_2/\text{CH}_3\text{OH}$ : 96:4 to 95:5).  $R_f$ : 0.36 ( $\text{CH}_2\text{Cl}_2/\text{CH}_3\text{OH}$ : 94:6);  $^1\text{H}$  NMR (400 MHz,  $\text{CD}_3\text{OD}$ )  $\delta$  8.01 (d,  $J=2.5$  Hz, 1H), 7.82 (dd,  $J=9.0$ , 2.5 Hz, 1H), 7.36-7.19 (m, 5H), 7.10 (d,  $J=9.0$  Hz, 1H), 5.35 (d,  $J=15.1$  Hz, 1H), 4.60-4.45 (m, 1H), 4.39 (d,  $J=6.8$  Hz, 1H), 4.14 (d,  $J=15.1$  Hz, 1H), 3.94 (s, 3H), 3.85 (t,  $J=4.0$  Hz, 1H), 3.77-3.54 (dd,  $J=16$ , 4 Hz, 2H), 3.07 (dd,  $J=14.6$ , 8.3 Hz, 1H), 2.80 (dd,  $J=14.6$ , 8.3 Hz, 1H), 2.27-2.22 (m, 1H), 2.10 (s, 3H), 1.45 (s, 9H), 1.06 (t,  $J=7.4$  Hz, 6H);  $^{13}\text{C}$  NMR (100 MHz,  $\text{CD}_3\text{OD}$ )  $\delta$  172.2, 171.7, 171.5, 167.8, 165.8, 158.0, 155.6, 129.9, 129.2, 128.9, 126.8, 124.2, 113.3, 60.5, 58.9, 56.9, 53.9, 48.5, 42.3, 41.9, 31.4, 28.8, 23.6, 19.7, 18.6; IR  $\nu_{\text{max}}$ : 3283, 2927, 1646, 1541, 1494, 1465, 1250, 1165, 1020; ESI+ MS  $m/z$  718.20  $[\text{M}+23]^+$ ; Anal. Calcd for  $\text{C}_{34}\text{H}_{45}\text{N}_7\text{O}_9 \cdot 1.5\text{H}_2\text{O}$ : C 56.49, H 6.71, N 13.57; found C 56.77, H 6.70, N 12.79.

#### Compound 6.

Compound 5 (0.172 mmol, 1 equiv) was deprotected according to general procedure A. The resulting TFA salt was then coupled to Boc-Ile-OH (0.26 mmol, 3 equiv) according to the general procedure B affording 7 (54 mg, 78%) as a white solid after purification by flash chromatography ( $\text{CH}_2\text{Cl}_2/\text{CH}_3\text{OH}$ : 95:5).  $R_f$ : 0.2 ( $\text{CH}_2\text{Cl}_2/\text{CH}_3\text{OH}$ : 94:6);  $^1\text{H}$  NMR (400 MHz,  $\text{CD}_3\text{OD}$ )  $\delta$  7.98 (d, 1H,  $J=2.5$  Hz), 7.83 (dd, 1H,  $J=9.0$ , 2.5 Hz), 7.46-7.25 (m, 5H), 7.11 (d, 1H,  $J=9.0$  Hz), 5.35 (d, 1H,  $J=15.1$  Hz), 4.54 (d, 1H,  $J=8.2$  Hz), 4.42 (t, 1H,  $J=4.2$  Hz), 4.28 (d, 1H,  $J=7.9$  Hz), 4.09-4.00 (m, 2H), 3.94 (s, 3H), 3.81 (dd, 2H,  $J=7.0$ , 4.1 Hz), 3.15 (dd, 1H,  $J=16.3$ , 4.2 Hz), 2.90 (dd, 1H,  $J=16.3$ , 4.2 Hz), 2.21-2.12 (m, 1H), 2.11 (s, 3H), 1.78-1.70 (m, 1H), 1.58-1.49 (m, 1H), 1.37 (s, 9H), 1.12 (d, 3H,  $J=6.8$  Hz), 1.06 (d, 3H,  $J=6.8$  Hz), 0.92-0.88 (m, 6H);  $^{13}\text{C}$  NMR (100 MHz,  $\text{CD}_3\text{OD}$ )  $\delta$  174.9, 172.1, 171.5, 171.4, 168.2, 167.3, 166.2, 157.8, 155.6, 136.8, 133.4, 129.9, 129.2, 129.0, 126.8, 124.3, 121.3, 113.3, 80.7, 60.1, 58.7, 58.4, 56.8, 53.2, 40.7, 39.1, 38.8, 32.0, 28.7, 25.9, 23.5, 19.6, 19.1, 16.2, 11.6; IR  $\nu_{\text{max}}$ : 3282, 2958, 2931, 1652, 1534, 1493, 1247, 1159, 737; HRMS Calc for  $\text{C}_{40}\text{H}_{56}\text{N}_8\text{O}_{10}$   $[\text{M}+\text{Na}]^+$  (831.4017): found 831.4019

#### Compound 7.

Compound 6 (0.056 mmol, 1 equiv) was deprotected according to general procedure A. The resulting TFA salt was coupled to Boc-Val (0.17 mmol, 3 equiv) according to the general procedure B affording 8 (42 mg, 83%) as a white solid after purification by flash chromatography ( $\text{CH}_2\text{Cl}_2/\text{CH}_3\text{OH}$ : 95:5).  $R_f$ : 0.15 ( $\text{CH}_2\text{Cl}_2/\text{CH}_3\text{OH}$ : 94:6); Mp 182-185 °C;  $^1\text{H}$  NMR

(400 MHz,  $\text{CD}_3\text{OD}$ )  $\delta$  8.05 (d,  $J=2.5$  Hz, 1H), 7.89 (dd,  $J=9.0$ , 2.5 Hz, 1H), 7.38-7.26 (m, 5H), 7.14 (d,  $J=9.0$  Hz, 1H), 5.39 (d,  $J=15.1$  Hz, 1H), 4.90 (d,  $J=8.5$  Hz, 1H), 4.68 (d,  $J=9.0$  Hz, 1H), 4.39 (t,  $J=4.2$  Hz, 1H), 4.08-4.05 (m, 1H), 4.03-3.96 (m, 4H ( $\text{CH}_3 + 1\text{H}$ )), 3.87 (dd,  $J=19.2$ , 6.4 Hz, 2H), 3.76-3.72 (m, 1H), 3.25 (dd,  $J=16.8$ , 4.7 Hz, 1H), 2.87 (dd,  $J=16.8$ , 4.7 Hz, 1H), 2.11 (s, 3H), 2.09-2.04 (m, 1H), 1.99-1.94 (m, 1H), 1.83-1.77 (m, 1H), 1.64-1.57 (m, 1H), 1.37 (s, 9H), 1.20-1.11 (m, 1H), 1.06-1.01 (m, 6H), 0.93-0.86 (m, 12H);  $^{13}\text{C}$  NMR (100 MHz,  $\text{CD}_3\text{OD}$ )  $\delta$  174.6, 174.2, 171.6, 171.1, 170.4, 168.4, 167.0, 164.2, 158.3, 155.6, 136.7, 133.7, 130.0, 129.2, 129.1, 127.0, 124.4, 120.9, 113.4, 80.4, 61.6, 58.7, 58.0, 57.8, 57.0, 53.1, 47.7, 40.3, 38.3, 38.2, 32.8, 31.8, 28.7, 28.0, 26.1, 23.6, 19.9, 19.7, 19.3, 18.8, 16.2, 11.5; IR  $\nu_{\text{max}}$ : 3314, 2946, 2833, 1653, 1541, 1495, 1249, 1165, 1025; HRMS Calc for  $\text{C}_{45}\text{H}_{65}\text{N}_9\text{NaO}_{11}$   $[\text{M}+\text{Na}]^+$  (930.4701): found 930.4697

#### Compound 8.

Compound 7 (0.028 mmol, 1 equiv) was deprotected according to general procedure A. The resulting TFA salt was coupled to Boc-Val (0.11 mmol, 3 equiv) according to the general procedure B affording 8 (21 mg, 74%) as a white solid after purification by flash chromatography ( $\text{CH}_2\text{Cl}_2/\text{CH}_3\text{OH}$ : 95:5).  $R_f$ : 0.2 ( $\text{CH}_2\text{Cl}_2/\text{CH}_3\text{OH}$ : 94:6);  $^1\text{H}$  NMR (400 MHz,  $\text{CD}_3\text{OD}$ )  $\delta$  8.10 (d,  $J=2.5$  Hz, 1H), 8.02 (dd,  $J=9.1$ , 2.5 Hz, 1H), 7.36-7.28 (m, 5H), 7.16 (d,  $J=9.1$  Hz, 1H), 5.41 (d,  $J=15.2$  Hz, 1H), 4.98 (d,  $J=8.5$  Hz, 1H), 4.76-4.71 (m, 1H), 4.39-4.42 (m, 2H), 4.13 (d,  $J=6.2$  Hz, 1H), 4.08 (d,  $J=4.4$  Hz, 1H), 4.03-3.97 (m, 4H), 3.92-3.88 (m, 1H), 3.77-3.69 (m, 2H), 3.30-3.28 (m, 1H), 2.88 (dd,  $J=17.2$ , 4.6 Hz, 1H), 2.11 (s, 3H), 2.08-2.01 (m, 2H), 1.99-1.92 (m, 1H), 1.83-1.76 (m, 1H), 1.59-1.52 (m, 1H), 1.41 (s, 9H), 1.15-1.07 (m, 1H), 1.02-0.98 (m, 6H), 0.93-0.83 (m, 18H);  $^{13}\text{C}$  NMR (100 MHz,  $\text{CD}_3\text{OD}$ )  $\delta$  174.2, 174.0, 173.5, 171.5, 171.1, 169.1, 168.4, 167.0, 162.5, 158.0, 155.5, 136.6, 133.8, 130.0, 129.2, 129.0, 127.2, 124.5, 124.4, 120.2, 113.5, 80.4, 61.1, 59.7, 58.6, 57.7, 57.2, 55.9, 52.9, 47.5, 43.8, 40.2, 38.3, 37.9, 33.0, 32.5, 31.9, 28.7, 26.2, 23.7, 19.9, 19.8, 19.6, 19.3, 19.0, 18.3, 17.3, 16.2, 13.1, 11.6; IR  $\nu_{\text{max}}$ : 3629, 1653, 1541, 779, 653; HRMS Calc for  $\text{C}_{50}\text{H}_{74}\text{N}_{10}\text{NaO}_{12}$   $[\text{M}+\text{Na}]^+$  (1029.5385): found 1029.5381.

#### Compound 9.

Compound 8 (0.028 mmol, 1 equiv) was deprotected according to general procedure A. The resulting TFA salt was coupled to Boc-Gly (0.11 mmol, 3 equiv) according to the general procedure B affording 9 (23 mg, 77%) as a light yellow solid after purification by flash chromatography ( $\text{CH}_2\text{Cl}_2/\text{CH}_3\text{OH}$ : 96:4 to 93:7).  $R_f$ : 0.2 ( $\text{CH}_2\text{Cl}_2/\text{CH}_3\text{OH}$ : 94:6);  $^1\text{H}$  NMR (400 MHz,  $\text{CD}_3\text{OD}$ )  $\delta$  8.29-8.24 (m, 2H), 7.35-7.28 (m, 5H), 7.17 (d,  $J=9.1$  Hz, 1H), 5.36 (d,  $J=15.2$  Hz, 1H), 5.01 (d,  $J=8.9$  Hz, 1H), 4.57 (d,  $J=7.3$  Hz, 1H), 4.44-4.37 (m, 1H), 4.12 (d,  $J=4.1$  Hz, 1H), 4.07-4.02 (m, 4H), 3.97-3.84 (m, 3H), 3.81-3.69 (m, 3H), 3.36-3.32 (m, 1H), 2.88 (dd,  $J=17.0$ , 4.1 Hz, 1H), 2.20 (s, 3H), 2.11-1.98 (m, 3H), 1.87-1.73 (m, 2H), 1.63-1.50 (m, 2H), 1.43 (s, 9H), 1.16-1.07 (m, 1H), 1.03-0.98 (m, 6H), 0.93-0.86 (m, 12H), 0.82-0.79 (m, 6H);  $^{13}\text{C}$  NMR (100 MHz,  $\text{CD}_3\text{OD}$ )  $\delta$



174.0, 173.0, 172.3, 171.7, 171.0, 168.6, 168.5, 167.0, 162.1, 155.4, 136.7, 134.3, 130.0, 129.2, 129.0, 126.8, 124.2, 119.5, 113.4, 80.5, 59.4, 59.1, 58.5, 57.7, 57.6, 57.2, 52.8, 47.6, 45.0, 42.9, 40.2, 38.4, 37.6, 33.4, 33.2, 33.1, 28.7, 26.3, 24.2, 19.7, 19.5, 19.4, 18.9, 16.3, 11.7; IR  $\nu_{\max}$ : 3293, 2967, 2926, 1641, 1630, 1551, 1364, 1225, 1159, 841; HRMS Calc for  $C_{52}H_{77}N_{11}NaO_{13}$  [M+Na]<sup>+</sup> (1086.5702): found 1086.5747.

### Compound 2.

Compound **9** (0.008 mmol, 1 equiv) was deprotected according to general procedure A affording **2** (8 mg, 66%) as a white solid. Mp 187-189 °C; <sup>1</sup>H NMR (400 MHz, CD<sub>3</sub>OD)  $\delta$  8.22 (d, 1H, J=4 Hz), 7.91 (dd, 1H, J=12.0, 4.0 Hz), 7.36-7.30 (m, 5H), 7.19 (d, 1H, J=12 Hz), 5.35 (d, 1H, J= 16 Hz), 4.97 (d, 1H, J=4 Hz), 4.63 (d, 1H, J=4 Hz), 4.48 (d, 1H, J=8 Hz), 4.41 (t, 1H, J=4Hz), 4.12-4.07 (m, 2H), 4.04 (s, 3H), 3.89-3.77 (m, 4H), 2.91-2.88 (m, 1H), 2.86-2.84 (m, 1H), 2.14 (s, 3H), 2.10-2.04 (m, 2H), 1.93-1.86 (m, 1H), 1.80-1.75 (m, 1H), 1.59-1.52 (m, 2H), 1.16-1.11 (m, 1H), 1.04-1.01 (m, 6H), 0.92-0.83 (m, 18H); <sup>13</sup>C NMR (100 MHz, CD<sub>3</sub>OD)  $\delta$  174.1, 173.0, 171.7, 171.2, 170.8, 169.4, 168.7, 168.5, 167.4, 167.0, 162.8, 155.7, 136.7, 133.8, 130.0, 129.2, 129.0, 127.2, 124.3, 120.1, 113.6, 65.1, 59.9, 59.8, 59.7, 58.5, 58.0, 57.8, 57.2, 54.7, 52.8, 47.7, 41.8, 40.2, 38.4, 37.9, 33.0, 32.9, 32.7, 32.5, 30.4, 26.1, 23.8, 19.8, 19.7, 19.6, 19.4, 19.2, 18.3, 16.2, 11.6; IR  $\nu_{\max}$ : 3278, 2968, 2936, 1642, 1624, 1544, 1469, 1290, 1130; HRMS (ESI<sup>+</sup>, MeOH): [M+Na]<sup>+</sup>.(986.5071): found  $m/z$ : 986.5075

### NMR spectroscopy.

Lyophilized **2** was dissolved at a concentration of 1.4 mM in 550  $\mu$ L of CD<sub>3</sub>OH (Eurisotop, Saint-Aubin, France). NMR experiments were recorded on a 500 MHz spectrometer equipped with a TCI <sup>1</sup>H/<sup>13</sup>C/<sup>15</sup>N cryoprobe. NMR spectra were processed with Topspin 2.0 software (Bruker) and analysed with Sparky program.<sup>22</sup> <sup>1</sup>H and <sup>13</sup>C resonances were completely assigned using 1D <sup>1</sup>H WATERGATE, 2D <sup>1</sup>H-<sup>1</sup>H TOCSY (MLEV17 isotropic scheme of 66 ms duration), 2D <sup>1</sup>H-<sup>1</sup>H ROESY (300 ms mixing time), 2D <sup>1</sup>H-<sup>13</sup>C HSQC, and 2D <sup>1</sup>H-<sup>13</sup>C HMBC spectra. <sup>1</sup>H and <sup>13</sup>C chemical shifts were calibrated using the solvent residual peak (CHD<sub>2</sub>OH,  $\delta$  <sup>1</sup>H 3.31 ppm,  $\delta$  <sup>13</sup>C 49.5 ppm). The chemical shift deviations were calculated as the differences between observed chemical shifts and random coil values reported in methanol for <sup>1</sup>H ( $\delta$  <sup>1</sup>H $\alpha$  4.23 ppm for Ile and 4.16 ppm for Val, unpublished data) and in water for <sup>13</sup>C resonances.<sup>18</sup> The temperature gradients of the amide proton chemical shifts were derived from 1D <sup>1</sup>H WATERGATE spectra recorded between 271 and 303 K. Vicinal coupling constants were extracted from 1D <sup>1</sup>H WATERGATE spectrum at 298 K. ROE cross-peaks were integrated using Sparky and converted into distances using the ROE correlation between the benzyl diastereotopic methylenic protons as a reference (1.8 Å).

### Computational methods.

Molecular mechanics studies were carried out using MacroModel from Schrödinger software suite.<sup>23</sup> An arbitrary

initial conformation of **1** was energy-minimized using conjugate gradient method<sup>24</sup> with OPLS\_2005 force field<sup>25</sup> and GBSA as an implicit water solvation model.<sup>26</sup> Convergence criterion was set to 0.05 kJ·mol<sup>-1</sup>·Å<sup>-1</sup> on energy gradient.

An unconstrained conformational search was then performed starting from this structure and using MCMM (Monte Carlo Multiple Minima) method<sup>27</sup> with the same force field, solvation model and convergence criterion. 100,000 conformations were generated, energy-minimized and deduplicated, resulting in 1583 unique conformations within a sliding energy window of 21 kJ/mol (~5 kcal/mol).

Clustering of these results using centroid linkage method with 0.66 Å merge distance threshold (as suggested by Kelley penalty function)<sup>28</sup> yielded 69 representative conformations. Conformations exhibiting the maximum number of hydrogen bonds participating in the structure of a hairpin (3 out of the 4 possible) were selected, and the most extended one (based on the radius of gyration with the benzyl group excluded) within this group was retained.

This conformation was subjected to a 1  $\mu$ s-long molecular dynamics at 310 K using the same force field and solvation model as above. Geometry optimization at the B3LYP/6-31G\* level<sup>29</sup> with water PCM solvation model<sup>30</sup> using Gaussian<sup>31</sup> was performed on the first frame where simultaneous formation of the 4 key hydrogen bonds occurred. <sup>3</sup>J(H<sup>N</sup>-H <sup>$\alpha$</sup> ) coupling constants were calculated according to the Karplus equation<sup>32</sup> from dihedral angles averaged over the trajectory. Figure 4 was plotted using gnuplot.<sup>33</sup> Figure 5 was prepared with PyMOL and rendered using POVRay.<sup>34</sup>

### Acknowledgements

We thank Fondazione CARIPLO (Project RE-D DRUG TRAIN 2010-1373: *Multidisciplinary approaches in research and development of innovative drugs: project for an international collaborative training network*) for a research grant (to U.P.) and a PhD fellowship to L.V. We also gratefully acknowledge Ministero dell'Università e della Ricerca for financial support (PRIN project 2010NRREPL). The IT department from Université Paris-Sud is acknowledged for providing computing resources. Claire Troufflard and Karine Leblanc (BioCIS, UMR 8076) are thanked for their help with the NMR experiments and HRMS and HPLC analysis respectively

### Notes and references

<sup>a</sup> Università degli Studi dell'Insubria, Dipartimento di Scienza e Alta Tecnologia, Via Valleggio 11, I-22100 Como, Italy.

\* Tel: +39 0312386444. Email: [Umberto.Piarulli@uninsubria.it](mailto:Umberto.Piarulli@uninsubria.it)

<sup>b</sup> Molécules Fluorées et Chimie Médicinale, BioCIS UMR-CNRS 8076, LabEx LERMIT, Université Paris-Sud, Faculté de Pharmacie, 5 rue Jean-Baptiste Clément, 92296 Châtenay-Malabry Cedex, France.

\* Tel : +33 146835737. E-mail: [Sandrine.Ongeri@u-psud.fr](mailto:Sandrine.Ongeri@u-psud.fr)

<sup>c</sup> Sorbonne Universités - UPMC Univ Paris 06, Ecole Normale Supérieure - PSL Research University, CNRS UMR 7203 LBM, 4 place Jussieu, 75252 Paris Cedex 05, France.

† Footnotes should appear here. These might include comments relevant to but not central to the matter under discussion, limited experimental and spectral data, and crystallographic data.

Electronic Supplementary Information (ESI) available: [details of any supplementary information available should be included here]. See DOI: 10.1039/b000000x/

- 1 a) G. M. Burslem, A. J. Wilson, *Synlett*, 2014, **25**, 324; b) M. K. P. Jayatunga, S. Thompson, A. D. Hamilton, *Bioorg. Med. Chem. Lett.*, 2014, **24**, 717; c) D. J. Hill, M. J. Mio, R. B. Prince, T. S. Hughes, J. S. Moore, *Chem. Rev.* 2001, **101**, 3893.
- 2 (a) P. N. Cheng, J. D. Pham, J. S. Nowick, *J. Am. Chem. Soc.*, 2013, **135**, 5477; (b) H. Remaut, G. Waksman, *Trends Biochem. Sci.*, 2006, **31**, 436.
- 3 M. Bartolini, V. Andrisano, *ChemBioChem*, 2010, **11**, 1018.
- 4 (a) B. Alberts, A. Johnson, J. Lewis, M. Raff, K. Roberts, P. Walter, *Molecular Biology of the Cell*, 5<sup>th</sup> ed, Garland Press: New York, 2007. (b) C. Branden, J. Tooze, *Introduction to Protein Structure*, 2<sup>nd</sup> ed, Garland Press: New York, 1999
- 5 (a) C. I. Stains, K. Mondal, I. Ghosh, *ChemMedChem*, 2007, **2**, 1674; (b) T. Liu, G. Bitan, *ChemMedChem*, 2012, **7**, 359; (c) B. Bulic, M. Pickhardt, E. Mandelkow, *J. Med. Chem.*, 2013, **56**, 4135.
- 6 (a) K. N. L. Huggins, M. Bisaglia, L. Bubacco, M. Taterek-Nossol, A. Kapurniotu, N. H. Andersen, *Biochemistry*, 2011, **50**, 8202; (b) J. Kellock, B. Caughey, V. Daggett, *ACS Med. Chem. Lett.*, 2013, **4**, 824; (c) G. Yamin, P. Ruchala, D. B. Teplow, *Biochemistry*, 2009, **48**, 11329; (d) Y. Murakoshi, T. Takahashi, H. Mihara, *Chem. Eur. J.*, 2013, **19**, 4525; (e) J. Luo, J. M. Otero, C. -H. Yu, S. K. T. S. Wärmländer, A. Gräslund, M. Overhand, J. P. Abrahams, *Chem. Eur. J.*, 2013, **19**, 17338.
- 7 (a) J. Zheng, C. Liu, M. R. Sawaya, B. Vadla, S. Khan, R. J. Woods, D. Eisenberg, W. J. Goux, J. S. Nowick, *J. Am. Chem. Soc.*, 2011, **133**, 3144; (b) P.-N. Cheng, C. Liu, M. Zhao, D. Eisenberg, J. S. Nowick, *Nature Chemistry*, 2012, **4**, 927.
- 8 (a) A. Ressurreição, A. Bordessa, M. Civera, L. Belvisi, C. Gennari, U. Piarulli, *J. Org. Chem.*, 2008, **73**, 652; (b) M. Marchini, M. Mingozzi, R. Colombo, C. Gennari, M. Durini, U. Piarulli, *Tetrahedron*, 2010, **66**, 9528.
- 9 R. Delatouche, M. Durini, M. Civera, L. Belvisi, U. Piarulli, *Tetrahedron Lett.*, 2010, **51**, 4278.
- 10 J. S. Nowick, D. M. Chung, K. Maitra, S. Maitra, K. D. Stigers, Y. Sun, *J. Am. Chem. Soc.*, 2000, **122**, 7654.
- 11 a) L. Bannwarth, A. Kessler, S. Pêthe, B. Collinet, N. Merabet, N. Boggetto, S. Sicsic, M. Reboud-Ravaux, S. Onger, *J. Med. Chem.*, 2006, **49**, 4657; b) A. Vidu, L. Dufau, L. Bannwarth, J-L Soulier, S. Sicsic, U. Piarulli, M. Reboud-Ravaux, S. Onger, *ChemMedChem.*, 2010, **5**, 1899.
- 12 D.L. Jr Minor, P.S. Kim, *Nature*, 1994, **367**, 660.
- 13 H. L. Rayle, L. Fellmeth, *Org. Process Res. Dev.*, 1999, **3**, 172.
- 14 C. A. G. N. Montalbetti, V. Falque, *Tetrahedron*, 2005, **61**, 10827.
- 15 Z. J. Kaminski, B. Kolesińska, J. Kolesińska, G. Sabatino, M. Chelli, P. Rovero, M. Błaszczuk, M. L. Głowska, A. Papini, *J. Am. Chem. Soc.*, 2005, **127**, 16912.
- 16 (a) P. G. Vasudev, S. Chatterjee, N. Shamala, P. Balaram, *Chem. Rev.*, 2011, **111**, 657; (b) D. Seebach, D. F. Hook, A. Glättli, *Biopolymers*, 2006, **84**, 23; (c) F. Fulop, T. A. Martinek, G. K. Tóth, *Chem. Soc. Rev.*, 2006, **35**, 323; (d) D. L. Steer, R. A. Lew, P. Perlmutter, A. I. Smith, M. I. Aguilar, *Curr. Med. Chem.*, 2002, **9**, 811; (e) R. P. Cheng, S. H. Gellman, W. F. DeGrado, *Chem. Rev.*, 2001, **101**, 3219.
- 17 D. Seebach, S. Abele, K. Gademann, B. Jaun, *Angew. Chem. Int. Ed.*, 1999, **38**, 1595.
- 18 a) D. S. Wishart, C G. Bigam, A. Holm, R. S Hodges, B. D. Sykes, *J. Biomol. NMR*. 1995, **5**, 67 ; b) C. M. Santiveri, E. León, M. Rico, M. A. Jiménez *Chem. Eur. J.* 2008, **14**, 488.
- 19 T. Cierpicki, J. Otlewski, *J. Biomol. NMR*, 2001, **21**, 249.
- 20 K. Guitot, M. Larregola, T. K. Pradhan J. L. Vasse, S. Lavielle, P. Bertus, J. Szymoniak, O. Lequin, P. Karoyan, *ChemBioChem*, 2011, **12**, 1039-1042
- 21 R. Zhou and B. J. Berne, *Proc. Natl. Acad. Sci. U. S. A.*, 2002, **99**, 12777.
- 22 T.D. Goddard, D. G. Kneller. Sparky 3, University of California, San Francisco. <http://www.cgl.ucsf.edu/home/sparky/>
- 23 MacroModel, version 10.2, Schrodinger, LLC, New York, NY, 2013.
- 24 E. Polak and G. Ribiere, *Revue française d'informatique et de recherche operationnelle*, 1969, **16**, 35.
- 25 The OPLS\_2005 parameters are described in J. L. Banks, H. S. Beard, Y. Cao, A. E. Cho, W. Damm, R. Farid, A. K. Felts, T. A. Halgren, D. T. Mainz, J. R. Maple, R. Murphy, D. M. Philipp, M. 2 P. Repasky, L. Y. Zhang, B. J. Berne, R. A. Friesner, E. Gallicchio and R. M. Levy, *J. Comp. Chem.* 2005, **26**, 1752.
- 26 W. C. Still, A. Tempczyk, R. C. Hawley and T. Hendrickson, *J. Am. Chem. Soc.*, 1990, **112**, 6127
- 27 G. Chang, W. C. Guida and W. Clark Still, *J. Am. Chem. Soc.*, 1989, **111**, 4379.
- 28 L. A. Kelley, S. P. Gardner and M. J. Sutcliffe, *Protein Eng.*, 1996, **9**, 1063

- 29 (a) W. Kohn, L. J. Sham, *Phys. Rev.*, 1965, **140**, A1133. (b) A. D. Becke, *J. Chem. Phys.*, 1993, **98**, 5648. (c) C. Lee, W. Yang, R. G. Parr, *Phys. Rev. B*, 1988, **37**, 785. (d) W. J. Hehre, L. Radom, P. v. R. Schleyer, J. A. Pople, *Ab Initio Molecular Orbital Theory*, Wiley, New York, 1986.
- 30 J. Tomasi, B. Mennucci and R. Cammi, *Chem. Rev.*, 2005, **105**, 999
- 31 M. J. Frisch, G. W. Trucks, H. B. Schlegel, G. E. Scuseria, M. A. Robb, J. R. Cheeseman, G. Scalmani, V. Barone, B. Mennucci, G. A. Petersson, H. Nakatsuji, M. Caricato, X. Li, H. P. Hratchian, A. F. Izmaylov, J. Bloino, G. Zheng, J. L. Sonnenberg, M. Hada, M. Ehara, K. Toyota, R. Fukuda, J. Hasegawa, M. Ishida, T. Nakajima, Y. Honda, O. Kitao, H. Nakai, T. Vreven, J. A. Montgomery Jr., J. E. Peralta, F. Ogliaro, M. Bearpark, J. J. Heyd, E. Brothers, K. N. Kudin, V. N. Staroverov, R. Kobayashi, J. Normand, K. Raghavachari, A. Rendell, J. C. Burant, S. S. Iyengar, J. Tomasi, M. Cossi, N. Rega, J. M. Millam, M. Klene, J. E. Knox, J. B. Cross, V. Bakken, C. Adamo, J. Jaramillo, R. Gomperts, R. E. Stratmann, O. Yazyev, A. J. Austin, R. Cammi, C. Pomelli, J. W. Ochterski, R. L. Martin, K. Morokuma, V. G. Zakrzewski, G. A. Voth, P. Salvador, J. J. Dannenberg, S. Dapprich, A. D. Daniels, Ö. Farkas, J. B. Foresman, J. V. Ortiz, J. Cioslowski and D. J. Fox, *Gaussian 09*, Revision A.02, Gaussian, Inc., Wallingford CT, 2009
- 32 G. W. Vuister and A. Bax, *J. Am. Chem. Soc.*, 1993, **115**, 7772.
- 33 Thomas Williams, Colin Kelley and many others, Gnuplot: an interactive plotting program, version 4.6, 2012. Available from <<http://www.gnuplot.info/>>.
- 34 Persistence of Vision Raytracer, version 3.7, Persistence of Vision Pty. Ltd., 2013. Available from <<http://www.povray.org/>>.